Comparative study of six antenna designs for receiving APT images from NOAA-19 in urban environments

Hernán Paz Penagos

https://orcid.org/0000-0002-2692-1989
hernan.paz@escuelaing.edu.co

Doctor en Educación
Docente e investigador – Universidad Escuela
Colombiana de Ingeniería Julio Garavito, Colombia
Rol del investigador: teórico y escritura
Grupo de Investigación ECITRONICA, Semillero de investigación AstroSpace

Ph.D. in Education
Teacher and Researcher - Universidad Escuela
Colombiana de Ingeniería Julio Garavito, Colombia
Researcher's role: theorist and writer
Researcher's role: theorist and writer ECITRONICA
Research Group, AstroSpace research group

Doutoramento em Educação
Docente e investigador - Universidad Escuela
Colombiana de Ingeniería Julio Garavito, Colômbia
Papel do investigador: teórico e escritor
Grupo de investigação ECITRONICA, grupo de investigação AstroSpace

Esteban Morales Mahecha

https://orcid.org/0009-0003-3897-0002
esteban.morales-m@mail.escuelaing.edu.co

Ingeniero Electrónico
Investigador – Universidad Escuela Colombiana
de Ingeniería Julio Garavito, Colombia
Rol del investigador: teórico y escritura
Grupo de Investigación ECITRONICA, Semillero de investigación AstroSpace

Electronic Engineering
Researcher – University Colombian School
of Engineering Julio Garavito, Colombia
Researcher's role: theoretical and writing
ECITRONICA Research Group, AstroSpace research group

Engenheiro eletrónico
Investigador - Universidad Escuela Colombiana
de Ingeniería Julio Garavito, Colômbia
Papel do investigador: teórico e escrito
Grupo de investigação ECITRONICA, grupo de investigação AstroSpace

Alejandro Páez Avendaño

https://orcid.org/0009-0005-8486-1952
ruben.campos@mail.escuelaing.edu.co

Ingeniero Electrónico
Investigador – Universidad Escuela Colombiana
de Ingeniería Julio Garavito, Colombia
Rol del investigador: teórico y escritura
Grupo de Investigación ECITRONICA, Semillero de investigación AstroSpace

Electronic Engineering
Researcher – University Colombian School
of Engineering Julio Garavito, Colombia
Researcher's role: theoretical and writing
ECITRONICA Research Group, AstroSpace research group

Engenheiro eletrónico
Investigador - Universidad Escuela Colombiana
de Ingeniería Julio Garavito, Colômbia
Papel do investigador: teórico e escrito
Grupo de investigação ECITRONICA, grupo de investigação AstroSpace

Rubén Campos Riaño

https://orcid.org/0009-0004-0119-9928
alejandro.paez@mail.escuelaing.edu.co

Ingeniero Electrónico
Investigador – Universidad Escuela Colombiana de
Ingeniería Julio Garavito, Colombia
Rol del investigador: teórico y escritura
Grupo de Investigación ECITRONICA, Semillero de investigación AstroSpace

Electronic Engineering
Researcher – University Colombian School
of Engineering Julio Garavito, Colombia
Researcher's role: theoretical and writing
ECITRONICA Research Group, AstroSpace research group

Engenheiro eletrónico
Investigador - Universidad Escuela Colombiana de
Ingeniería Julio Garavito, Colômbia
Papel do investigador: teórico e escrito
Grupo de investigação ECITRONICA, grupo de investigação AstroSpace

Comparative study of six antenna designs for receiving APT images from NOAA-19 in urban environments

Abstract: The objective of this article is to design, build, test, and compare the performance of six antennas (Turnstile, QHF, double-cross, Moxon, V-dipole, and Eggbeater) used for receiving APT meteorological images transmitted from the NOAA-19 satellite in an urban environment. The process follows a four-phase methodology: research, tuning system development, design and simulation, construction, and testing. During the research phase, fundamental concepts such as RTL-SDR, NOAA satellites, and the APT format for image transmission are explored. Subsequently, the development of the tuning system involves the use of programs such as SDRsharp and WXtoImg to receive and decode the APT signal. The next phase encompasses the design, simulation, and construction of the antennas, with the selection of NOAA satellites. Virtual tools are employed to calculate dimensions and parameters, followed by the assembly of the antenna designs. Tests are conducted in open spaces, aligning with the satellite orbits, to receive images. Finally, the results are evaluated in terms of image resolution and audio power to determine the most suitable antenna arrays for this type of communication. The Moxon antenna emerged as the best-performing, recovering images with resolutions of 1.94 megapixels, while the QHF antenna exhibited the highest power reception at 1.9 W. The V-dipole, QHF, and Eggbeater antennas demonstrated the best coupling with the transmission line, achieving low reflection coefficients of 0.16. In conclusion, it is established that in urban environments, the Moxon and QHF antennas effectively receive APT images.

Keywords: APT, NOAA-19 satellite, meteorological images, RTL-SDR.

Estudio comparativo de seis diseños de antenas para la recepción de imágenes APT NOAA-19 en entornos urbanos

Resumen: El objetivo de este artículo es diseñar, construir, probar y comparar el rendimiento de seis antenas (Turnstile, QHF, double-cross, Moxon, V-dipole y Eggbeater) utilizadas para recibir imágenes meteorológicas APT transmitidas desde el satélite NOAA-19 en un entorno urbano. El proceso sigue una metodología de cuatro fases: investigación, desarrollo del sistema de sintonización, diseño y simulación, construcción y prueba. Durante la fase de investigación, se exploran conceptos fundamentales como RTL-SDR, satélites NOAA y el formato APT para la transmisión de imágenes. Posteriormente, el desarrollo del sistema de sintonización implica el uso de programas como SDRsharp y WXtoImg para recibir y decodificar la señal APT. La siguiente fase abarca el diseño, simulación y construcción de las antenas, con la selección de satélites NOAA. Se emplean herramientas virtuales para calcular dimensiones y parámetros, seguidas por el ensamblaje de los diseños de las antenas. Se realizan pruebas en espacios abiertos, alineándose con las órbitas de los satélites, para recibir imágenes. Finalmente, los resultados se evalúan en términos de resolución de imagen y potencia de audio para determinar las matrices de antenas más adecuadas para este tipo de comunicación. La antena Moxon surgió como la de mejor rendimiento, recuperando imágenes con resoluciones de 1.94 megapíxeles, mientras que la antena QHF exhibió la mayor recepción de potencia a 1.9 W. Las antenas V-dipole, QHF y Eggbeater demostraron el mejor acoplamiento con la línea de transmisión, logrando coeficientes de reflexión bajos de 0.16. En conclusión, se establece que, en entornos urbanos, las antenas Moxon y QHF reciben eficazmente imágenes APT.

Palabras clave: APT, satélite NOAA-19, imágenes meteorológicas, RTL-SDR.

Estudo comparativo de seis projetos de antenas para recepção de imagens APT NOAA-19 em ambientes urbanos

Resumo: O objetivo deste artigo é projetar, construir, testar e comparar o desempenho de seis antenas (Turnstile, QHF, double-cross, Moxon, V-dipole e Eggbeater) usadas para receber imagens meteorológicas APT transmitidas do satélite NOAA-19 em um ambiente urbano. O processo segue uma metodologia de quatro fases: pesquisa, desenvolvimento do sistema de sintonia, design e simulação, construção e teste. Durante a fase de pesquisa, são explorados conceitos fundamentais como RTL-SDR, satélites NOAA e o formato APT para transmissão de imagens. Posteriormente, o desenvolvimento do sistema de sintonia envolve o uso de programas como SDRsharp e WXtoImg para receber e decodificar o sinal APT. A próxima fase abrange o design, simulação e construção das antenas, com a seleção dos satélites NOAA. Ferramentas virtuais são empregadas para calcular dimensões e parâmetros, seguidas pela montagem dos designs das antenas. Testes são conduzidos em espaços abertos, alinhando-se com as órbitas dos satélites, para receber imagens. Finalmente, os resultados são avaliados em termos de resolução de imagem e potência de áudio para determinar as matrizes de antenas mais adequadas para esse tipo de comunicação. A antena Moxon destacou-se como a de melhor desempenho, recuperando imagens com resoluções de 1,94 megapixels, enquanto a antena QHF exibiu a maior recepção de potência, com 1,9 W. As antenas V-dipole, QHF e Eggbeater demonstraram o melhor acoplamento com a linha de transmissão, atingindo coeficientes de reflexão baixos de 0,16. Em conclusão, estabelece-se que, em ambientes urbanos, as antenas Moxon e QHF recebem efetivamente imagens APT.

Palavras-chave: APT, satélite NOAA-19, imagens meteorológicas, RTL-SDR.

Introduction

Receiving images from meteorological satellites has become indispensable for various fields, ranging from weather forecasting to natural disaster management. Satellites operated by the United States National Oceanic and Atmospheric Administration (NOAA) play a crucial role in providing these valuable images globally. NOAA, a United States scientific agency, primarily focuses on the global monitoring of oceans and the atmosphere through its satellites. The satellites used in this study, namely NOAA-15, 18, and 19, are positioned in low polar orbits between 800 and 1500 km above the Earth's surface. They utilize high-frequency transmitters in the 137 MHz band to transmit collected data. Employing the APT (Automatic Picture Transmission) transmission format, these satellites encode captured images in amplitude modulation (Bosquez, 2016). With the RTL-SDR module, the carrier frequencies are tuned, and the WXtoImg software facilitates the decoding of APT signals into PNG images (Velasco & Tipantuña, 2017). SDR technology provides a cost-effective solution for tracking small satellites, thereby reducing ground station development and implementation costs (Peralta *et al.*, 2018).

A critical factor influencing the reception of NOAA satellite signals is the choice of antenna. The selection of an appropriate antenna significantly impacts the quality of received images. While the literature includes publications on antennas utilized for receiving images from NOAA satellites, analyzing their performance compared to one or two other antennas, it does not comprehensively cover a larger number of antennas, as noted by the authors (Bosquez, 2016; Velasco & Tupantuña, 2017). This article aims to answer the question: What is the most suitable design for a low-cost, quickly constructible antenna that can be easily implemented and operated by university students for effective reception of images from NOAA satellites in urban environments? To address this inquiry, we compare various antennas and evaluate the results to determine the optimal choice for this application.

Methodology

For the Transmission Media course (METX) within the study plan of the Electronic Engineering program, the instructor assigned a laboratory project to the students. This project involved assigning the study, characterization, and construction of a different type of antenna to each group in the course. Ten laboratory groups, each consisting of three members, worked on the design of the following antennas: Turnstile antenna, QHF antenna, double-cross antenna, Moxon antenna, V-dipole, and Eggbeater.

The following flowchart in Figure 1 illustrates the methodological design of the laboratory practice divided into specific phases.

In the research phase (Figure 2), each laboratory group consulted and studied the most relevant concepts related to RTL-SDR and its operation, the set of NOAA satellites, and their utilization for the study of data transmission. Additionally, the definition of the format through which the satellites transmit analog images (APT) was explored.

After acquiring the relevant information and comprehending the concepts, the groups proceeded to configure the receiving system for tuning, as shown in Figure 3.
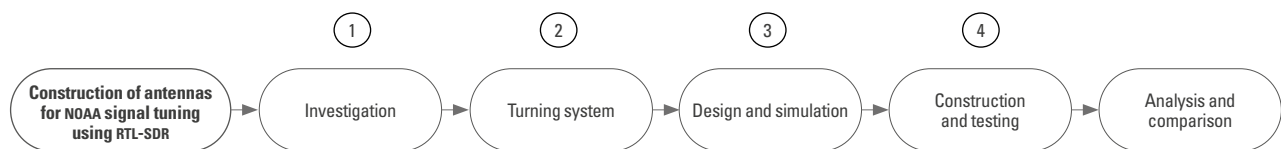
Construction of antennas for NOAA signal tuning using RTL-SDR → ① Investigation → ② Turning system → ③ Design and simulation → ④ Construction and testing → Analysis and comparison

Figure 1. General flow diagram of the method followed
Source: Own elaboration.

Comparative study of six antenna designs for receiving APT images from NOAA-19 in urban environments
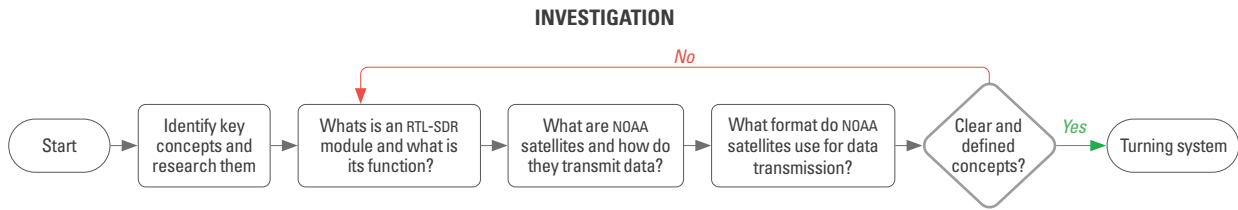
INVESTIGATION

Figure 2. Flow diagram of the investigation
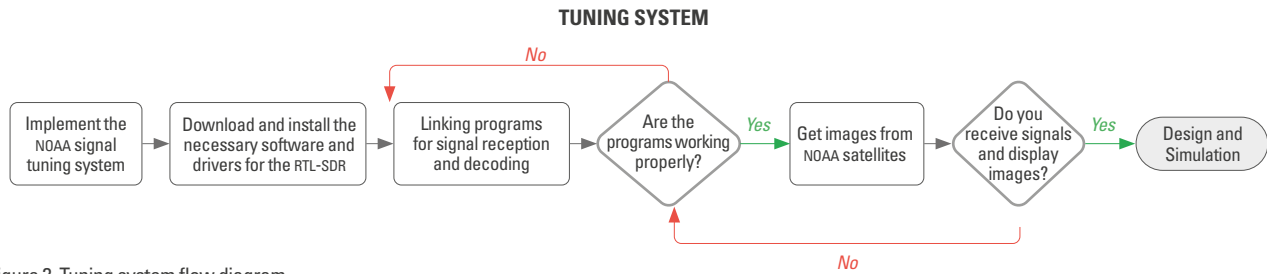Source: own elaboration.

TUNING SYSTEM

Figure 3. Tuning system flow diagram
Source: Own elaboration.

To enable the tuning system, it is necessary to install and link the SDRsharp and WXtoImg programs for receiving and decoding the audio signal in APT format. Since the receiver is designed on a software-defined radio (RTL-SDR), it is essential to download the required drivers for its operation. This design aims to visualize the carrier signal on a computer using the SDRsharp software, thus confirming the functionality of the signal tuning system. Subsequently, the WXto-Img software is employed to demodulate and recover the received audio or image. Phase three, shown in Figure 4, consisted of the design and simulation of the antennas mentioned.

For this phase, the students selected the NOAA satellite to tune, as each satellite operates on a specific frequency for data transmission, forming the basis for antenna design. Due to the course's nature, students possessed prior theoretical knowledge of antenna design. Consequently, they conducted a comprehensive review of the theory for each antenna type, identifying and determining the corresponding parameters for the design. Utilizing virtual design tools, the students calculated the dimensions and specifications of the antenna. In the case of simpler antennas, some students proceeded directly to construction. They verified the radiation pattern, directivity, and impedance of their designed antennas using the collected data through simulation.

Figure 5 shows the construction and testing phase of the receiving antenna for NOAA signal tuning using an RTL-SDR module.
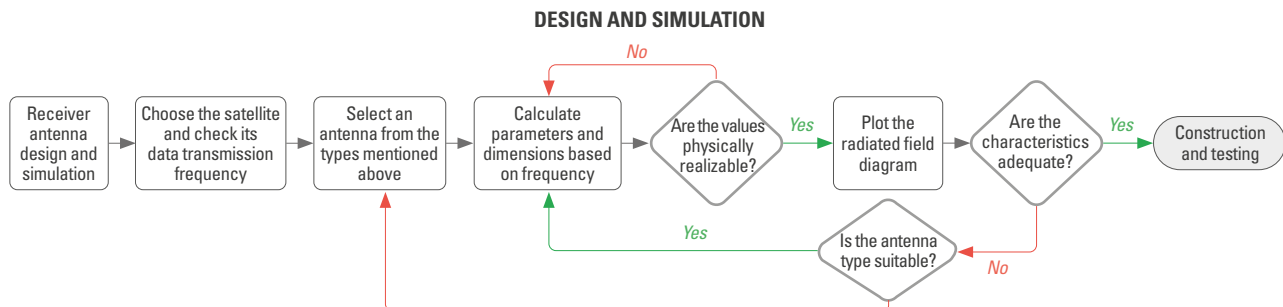
DESIGN AND SIMULATION

Figure 4. Design and simulation flow diagram
Source: Own elaboration.
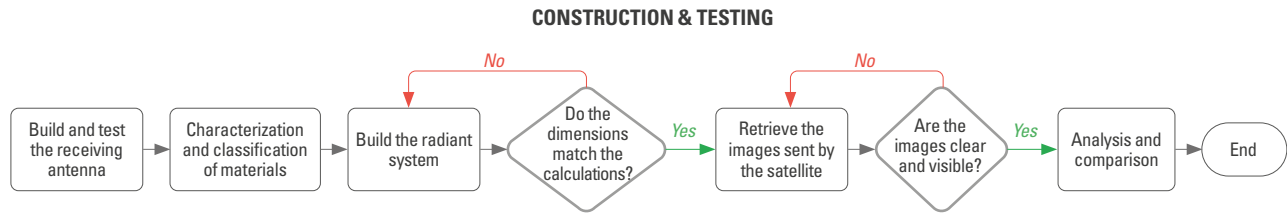
CONSTRUCTION & TESTING

Figure 5. Construction and testing flow diagram
Source: Own elaboration.

Using their theoretical designs as a basis, the students classified and identified the recyclable materials intended for constructing their radiant system. They utilized recycled low-gauge copper pipes, wood, PVC (polyvinyl chloride) pipes, and joints for the antenna. The transmission line and tuning system were constructed using coaxial cable, SMA (Subminiature version A) connectors, a computer, and an RTL-SDR module. The selection of these materials adhered to specific criteria: recyclability, easy accessibility, and low cost.

Then, they consulted the schedules in which the satellites performed their respective orbits, and which coincided with the coordinates of Bogota (4°46'56"N 74°02'38"O / 4.78222, -74.0439), where the tests were carried out. The laboratory groups looked for open and clear spaces, with acceptable weather conditions to obtain better results.

In this phase, researchers identify both successes and failures resulting from the precision or lack thereof in antenna construction. Deviating too far from the theoretical measurements directly impacts the antenna's resonance frequency, leading to inadequate reception of NOAA signals. Additionally, poor impedance coupling between the antenna and the transmission line negatively influences data reception.

To ensure rigor and quality in the design and manufacturing of the antennas, uniform specifications and recyclable materials were employed for all antennas, utilizing the same manufacturing elements (aluminum, PVC, and 75 Ω coaxial cable). Likewise, all antennas were specifically designed for reception at the 137.1 MHz frequency of the NOAA-19 satellite. To enhance data comparability, tests were conducted simultaneously at a single geographic site, under the same environmental conditions.

Each working group compared the data received based on criteria such as image resolution and peak audio power. This comparison aimed to inform a decision regarding the most suitable type of antenna for receiving this type of communication.

Results

As mentioned above, the evaluation of the images was performed taking into account the resolution in megapixels, which was calculated using the number of pixels in the vertical and horizontal dimensions. A higher number of megapixels and pixels was interpreted as better image reception.

On the other hand, the audio of the carrier signal, which contained the transmitted image information, was analyzed through SDRsharp and Python COLAB software. The Fourier function was studied and the power spectrum of the audio was examined. The peak power of the audio was used as an indicator of the quality of the received signal. Higher peak power was considered as a better quality signal. The captured images are shown in Figure 6.

Figure 1a shows the image taken by the Turnstile antenna; Figure 1b shows the image corresponding to the QHF antenna, while Figure 1c shows the image captured by the double-cross antenna. The image obtained by the Moxon antenna is shown in Figure 1d, with the V-dipole antenna the image presented in Figure 1e. Finally, Figure 1f shows the image received by the Eggbeater antenna. The information on the resolution and peak power of the audio corresponding to the six antennas is shown in Table 1.
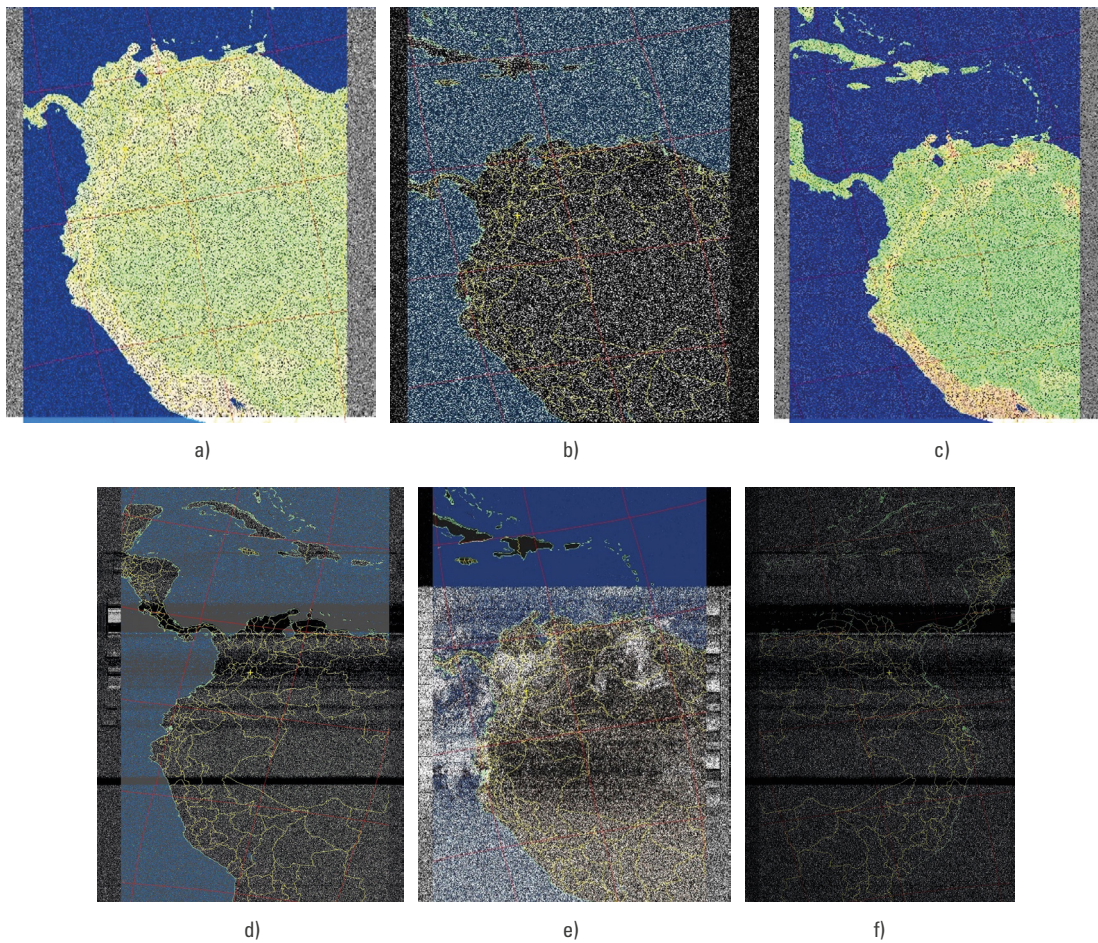
Figure 6. Images captured by the different antennas

Source: Own elaboration.

Table 1.
Comparative table of results obtained by each antenna

Image	Resolution (megapixels)	Pixels on vertical axis	Pixels on horizontal axis	Recovered signal peak power (mW)
1a	1,41544	1361	1040	863,23
1b	1,08056	1039	1040	1920,3
1c	1,4612	1405	1040	3,33
1d	1,93648	1862	1040	2,47
1e	1,43832	1383	1040	1264
1f	1,515544	1556	974	141,63

Source: Own elaboration.

Image 1d, captured using the Moxon antenna, stands out as the highest resolution image, reaching 1.93648 megapixels. This suggests that the Moxon antenna is suitable for obtaining detailed and clear images. In contrast, image 1b, from the QHF antenna, stands out as exhibiting the highest carrier audio power, registering 1.9 W. Despite having a slightly lower resolution, the QHF antenna proves to be adequate in receiving weak signals. These findings highlight the particularities of the antennas in question.

Analysis of results

NOAA satellites orbit in a polar orbit, so they appear in azimuth and elevation directions from any terrestrial location. Consequently, to receive APT signals

originating from these satellites, it is recommended to use receiving antennas with right-hand circular polarization (RHCP) and terrestrial radiation patterns with a minimum of nulls within the hemisphere, and a maximum in all directions in the horizontal plane. For this reason, antennas such as double-cross, QHF, Turnstile in axial mode, Moxon, V-dipole, and Eggbeater were selected, as shown in the following figures.

Delving into the topic, the Turnstile antenna in axial mode consists of a set of two half-wavelength dipoles aligned at right angles to each other; the currents in the dipoles have equal magnitude and are phase-shifted by 90°. The antenna is supported by a mast. The radiation pattern is omnidirectional with a null along the X-axis. To further enhance the shape of the horizontal pattern, additional elements are placed in a vertical array; with this type of antenna, the bandwidth can be expanded, gain improved, and polarization controlled; in addition to its ease of installation. See Figure 7 to learn about its radiation pattern.
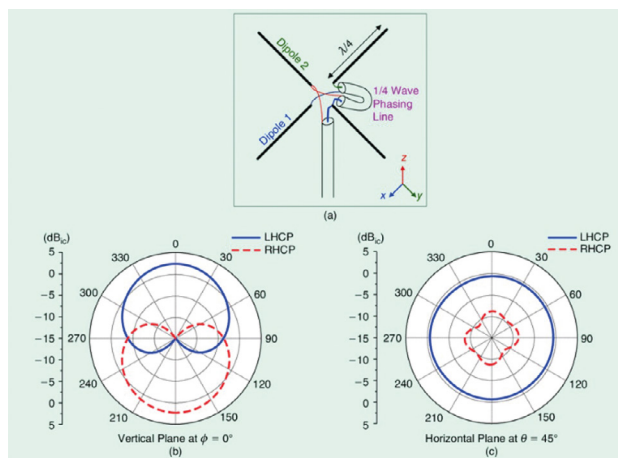

Figure 7. Radiation pattern of a Turnstile antenna
Source: Ta *et al.* (2015).

In contrast to the Turnstile, the QHF antenna has circularity in its entire reception area; it is formed by two linear conductors forming a helix, this shape is made to achieve circular polarization. The quality of the antenna reception depended largely on the quality of the joints and the symmetry that this antenna maintained in its final arrangement. The diameter-to-height ratio of the antenna was 0.44; however, if it is built

taller and narrower, the directivity of the antenna can be improved, thus receiving better signals from satellites near the horizon. The radiation pattern can be appreciated in the following image (Figure 8).
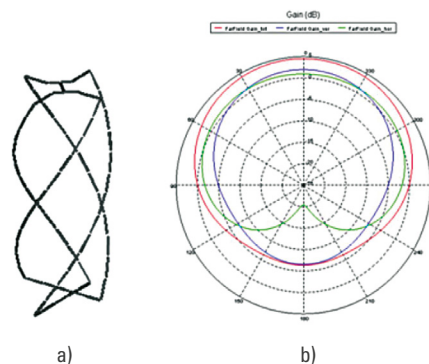

Figure 8. The geometry with wire segments a) and simulated radiation patterns b) of QHA
Source: Blazevic and Skiljo (2011).

On the other hand, the double-cross antenna consists of two sets of two half-wavelength dipoles aligned at right angles to each other. The omnidirectional pattern, which can be seen in Figure 9, has characteristics of circularly symmetric radiation (almost isotropic: 0 dBi is maintained in almost all directions in the entire 3-D space) and with greater horizontal directivity. This behavior is attributed to the fact that the two dipoles of each cross perform an omnidirectional pattern in the horizontal plane; while the set of the two crosses leads to a radiation pattern expanded to the vertical plane, due to their separation by a quarter wavelength. Field tests with this antenna indicate that it produces very little radiation pattern nulling within the hemisphere.

The Moxon antenna consists of two squares crossed at right angles and electrically phased 90° to obtain circular polarization. This antenna differs from the Turnstile in the shape of its radiation lobe; generally it is presented that for elevation angles between 90° and 70° the Turnstile outperforms the Moxon, between 70° and 40° they perform similarly, and for elevation angles less than 40° the Moxon outperforms the Turnstile. The radiation pattern of the same can be seen in Figure 10.
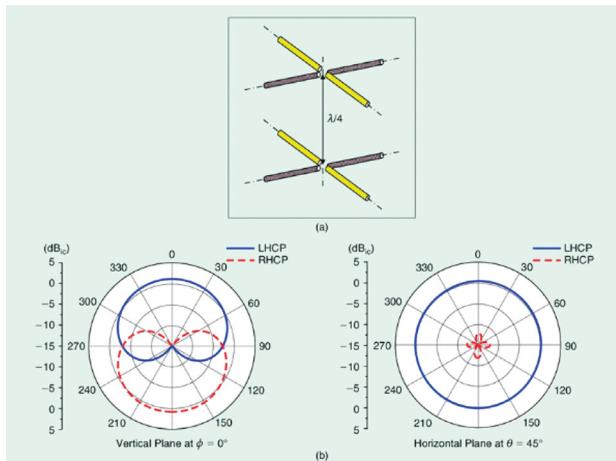
Figure 9. A double-Turnstile antenna in free space. (a) The 3-D view and (b) its radiation pattern at the resonant frequency
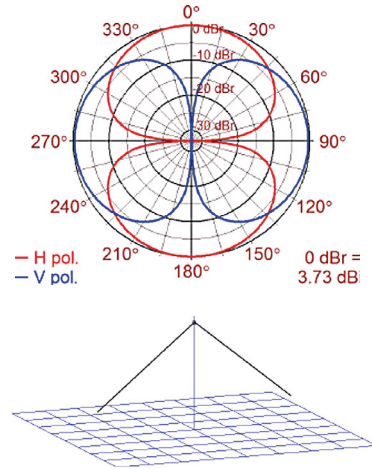Source: Ta *et al.* (2015).

Figure 11. Hemisphere polarization graph of the inverted vee half-wave dipole antenna at a height of 0.21 λ, and inverted vee half-wave dipole antenna, requiring only one support. Apex height is 0.21 λ, end height is 0.05 λ
Source: Witvliet *et al.* (2015).

Finally, the Eggbeater antenna consists of two loops phased 90° and the reflector elements that form the ground plane; its radiation pattern is omnidirectional, and can be appreciate in Figure 12, and its performance is good for receiving LEO satellite signals, although it does not reach the gain of the QFH; below 20° elevation, better performance is achieved than with the QFH. From 20° elevation, a better signal is usually obtained with the QFH.
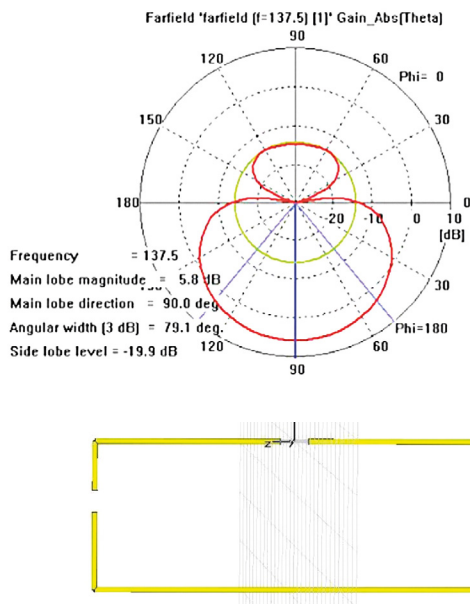

Figure 10. Image edited. Radiation pattern diagram for 137MHz and BW = 2.4GHz of a Moxon antenna, and Moxon antenna simulation in CST
Source: Cimino-Quiñones (2015).

The V-dipole antenna is formed by two linear conductors with a half-wavelength length and separated by 120°. It has a low gain of 2.15 dBi and an omnidirectional radiation pattern, which can be seen represented in Figure 11, its polarization is linear, so it presents losses due to polarization since the APT signal has RHCP polarization.
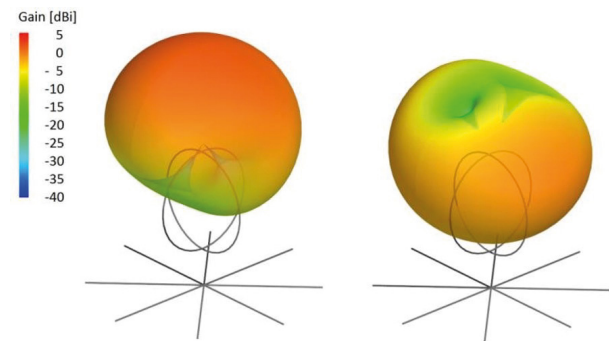

Figure 12. Calculated radiation patterns with Antenna Magus. Left: RHCP, right: LHCP
Source: Jain *et al.* (2018) and Hauer *et al.* (2018).

Taking the above into account, analyzing the performance results of the six antennas presented in Table 1, the values of the compared parameters enable

the identification of the Moxon antenna as the most effective antenna for NOAA signal reception, as indicated in Table 2.

In comparison, the Moxon antenna demonstrated the best performance, recovering images with resolutions of 1.94 megapixels. The QHF antenna exhibited the highest power reception at 1.9 W. The V-dipole, QHF, and Eggbeater antennas displayed the best coupling with the transmission line, achieving low reflection coefficients of 0.16. All antennas adhered to the transmission line length of λ/4.

All antennas, except the Moxon, evidenced circular polarization, which generally has an extra 3 dB loss due to polarization mismatch. Some disadvantages of the Turnstile antenna are: poor performance near the horizon, high image quality in a +/-30° approximately vertical field of view, and its radiation power is about 3 dB less compared to the maximum of a half-wave dipole radiating the same power.

When using reception antennas that are sensitive only to RHCP fields, the reception of electromagnetic waves reflected on the ground and suggesting left-hand circular polarization (LHCP) is not taken into account, particularly in the reception of all electromagnetic waves coming from the horizontal direction.

The receiving antennas studied were all mounted in the same fixed azimuthal position and with the same pointing (at the satellite) to be able to track the satellite during its pass. However, the appearance of the satellite in the azimuthal and elevation direction did not always coincide with what was budgeted. In one of the tests, it was observed that when the satellite was located at the highest and closest point, where the antennas should have a minimum of 12 dB towards the zenith, since theoretically the satellites are 12 dB stronger when they are high compared to their strength when they are on the horizon due to path loss, the Moxon antenna performed the best during the satellite pass, because it had lower gain at the most favorable moment (high and close satellite) and higher gain at the most unfavorable moment (low and distant satellite).

In addition, NOAA satellites orbit at an average altitude of 800 km, which provides between 12 and 15 minutes of signal reception on the ground; however, the range of best signal reception is approximately 8 minutes.

Table 2.
Comparative table of technical characteristics of the antennas

Antenna type	Comparison parameter					
	Input impedance	Bandwidth	Radiation pattern	Recommended operating band	Level of difficulty in design and construction	Polarization of the electromagnetic wave
Turnstile Antenna (axial mode)	36 Ω. This value produces an SWR between 1.3:1 and 1.4:1 at the feed point.	Broadband	Omnidirectional, no nulls along the axial direction (boresight).	Used for VHF communications, FM and TV transmissions, military and satellite communications.	The axial mode is of medium complexity, consisting of a combination of two orthogonal dipoles fed with equal amplitudes and phase in quadrature.	Circular
QHF Antenna	At resonance from 50 to 75 Ω	Narrow band	Omnidirectional	The QFH is an excellent antenna for meteorological satellites.	Complex	Circular
Antenna Double-Cross Antenna	73+42.5 Ω	Narrow band	Omnidirectional	VHF communications	High (complex)	Circular
Antenna Moxon	75 Ω, no Balun required	Narrow band	With a directive gain of up to 9.7 dBi at 28 MHz, the antenna can be achieved	VHF communications	Low complexity	Circular
V-Dipole	51.6 Ω	Broadband	Directive	Ham Radio	Low (simple)	Linear vertical or horizontal
Eggbeater	50 Ω	Narrow band	Omnidirectional	Receives VHF and UHF signals, ham radio.	Medium complexity	Circular

Source: Own elaboration.

Conclusions

In urban environments, the Moxon and QHF antennas excel in the reception of APT images sent from the NOAA-19 satellite. The Moxon antenna exhibits adequate performance in the resolution of the received signals, managing to recover images with a quality of 1.94 megapixels, while the QHF antenna tunes the highest power of 1.9 W.

For optimal reception of polar satellites, non-directional antennas with large capture area and circular polarization are required, such as the Turnstile, QHF and double-cross antennas. Although the Turnstile has good performance, it has limitations at the horizon and elevations outside +/-30°. Most are omnidirectional in azimuth, but some like the Turnstile perform better at low elevations. In general, the non-directional ones like QHF and double-cross are better choices for polar satellite reception without the need to adjust angles.

Although the antennas utilized in this study were not constructed to the highest standards, they offer a clear comparison under the same criteria of the performance of each antenna. It is acknowledged that each antenna has the potential for improvement to minimize noise, distortions, etc.

After conducting a thorough literature review, it is evident that our study presents a novel approach and scope not previously addressed. While some similar information exists in other articles, these works focus on different aspects or use different antenna configurations. For instance, one study developed a meteorological monitoring prototype using a different antenna and Raspberry Pi 3, while our study compares six types of antennas for receiving NOAA signals. Similarly, another study focused on a ground station prototype using different technology. Therefore, our study makes a significant contribution to the field by evaluating antennas under specific conditions. This highlights the originality and relevance of our work, offering new insights into antenna effectiveness in urban environments for receiving NOAA signals. Further research in this area is warranted.

References

Álvarez-Busani, C. (2012). *Diseño y construcción de una antena double cross para recepción de imágenes procedentes de satélites de órbita polar* (master dissertation, Universidad Politécnica de Cataluña). https://tinyurl.com/mwdv2mye

Balanis, C. A. (2005). *Antenna Theory: Analysis and Design* (3rd ed.). Wiley.

Blazevic, Z. & Skiljo, M. (2011). Helical Antennas in Satellite Radio Channel. *Advances in Satellite Communications* (M. Karimi & Y. Labrador, eds.). InTechOpen. https://doi.org/10.5772/21833

Bosquez, C. (2016). System for Receiving NOAA Meteorological Satellite Images using Software Defined Radio [paper]. *2016 IEEE ANDESCON*. Arequipa, Perú, 19-21 October 2016. https://doi.org/10.1109/ANDESCON.2016.7836233

Cimino-Quiñones, L., Stable-Sánchez, Y. & Valdés-Abreu, J. C. (2015). Antena MOXON para estaciones terrenas de satélites meteorológicos de órbita polar. *Ingeniería Electrónica, Automática y Comunicaciones, 36*(1), 79-94.

Hauer, L.-C., Fexer, S., Smolko, A., Struss, M., Solmaz, P., Munzel, T. & Thienel, T.-H. (2018). *Mobile Ground Station for CubeSat Operations* [en línea]. https://tinyurl.com/3vpvysnz

Jain, A., Chavan, P., Maradiya, P. & Rathod, K. (2018). Performance Investigation of Dipole and Moxon Antennae for VHF Communication. *Progress in Advanced Computing and Intelligent Engineering* (K. Saeed, N. Chaki, B. Pati, S. Bakshi & D. Prasad Mohapatra, eds.). Springer.

Mahmood, S., Mushtaq, M. T. & Jaffer, G. (2016). Cost Efficient Design Approach for Receiving the NOAA Weather Satellites Data. *2016 IEEE Aerospace Conference*. Big Sky, Montana, USA, 05-12 March 2016. https://doi.org/10.1109/AERO.2016.7500854

Martes, G. (2008). *Double Cross — A NOAA Satellite Downlink Antenna*. https://www.qsl.net/py4zbz/DCA.pdf

Patil, C., Chavan, T. & Chaudhari, M. (2016). Hardware and Software Implementation of Weather Satellite Imaging Earth Station. *2016 International Conference on Advances in Computing, Communications and Informatics (ICACCI)*. Jaipur, India, 21-24 September 2016. https://doi.org/10.1109/ICACCI.2016.7732122

Peralta, D. J. M., Dos Santos, D. S., Tikami, A., Dos Santos, W. A. & Pereira E. W. R. (2018). Satellite Telemetry and Image Reception with Software Defined Radio Applied to

Escuela de Postgrados de la **Fuerza Aérea Colombiana**

Space Outreach Projects in Brazil. *Anais da Academia Brasileira de Ciencias, 90*(3), 3175-3184. https://doi.org/10.1590/0001-3765201820170955

Ramos-Rosero, A. G. & Noboa-Cabrera, L. N. (2017). *Diseño e implementación de un prototipo para recepción de señales satelitales para obtención de imágenes meteorológicas del sistema de satélites NOAA (National Oceanic and Atmospheric Administration) usando radio definido por software* (tesis de grado, Universidad Politécnica Salesiana). Repositorio institucional. https://tinyurl.com/ykjdh8a5

Rojas Molina, R.D. (2019). *Diseñar un prototipo para recepción de imágenes APT (Automatic Picture Transmission) del sistema satelital NOAA (National Oceanic and Atmospheric Administration) usando RTL-SDR* (tesis de maestría, Universidad Israel). Repositorio institucional UIsrael. https://tinyurl.com/jmjh8j7v

Suarez-Fajardo, C.A., Ariza-Pulido, J. J., Mejía-Serrano, S. E. & Puerto-Leguizamón, G. A. (2017). Antena de placa suspendida con polarización circular y sentido de giro configurable. *INGE CUC, 16*(1), 156-170. http://doi.org/10.17981/ingecuc.16.1.2020.011

Ta, S. X., Park, I. & Ziolkowski, R. W. (2015). Crossed Dipole Antennas: A Review. *IEEE Antennas and Propagation Magazine, 57*(5), 107-122. https://doi.org/10.1109/MAP.2015.2470680

Tsai, L. C., Tien, M. H., Chen, G.H. & Zhang, Y. (2014). HF radio angle-of-arrival measurements and ionosonde positioning. *Terrestrial, Atmospheric and Oceanic Sciences, 25*(3), 401-413. https://doi.org/10.3319/TAO.2013.12.19.01(AA)

Velasco, C. & Tipantuña, C. (2017). Meteorological Picture Reception System using Software Defined Radio (SDR). *2017 IEEE Second Ecuador Technical Chapters Meeting (ETCM)*. Salinas, Ecuador, 16-20 October 2017. https://doi.org/10.1109/ETCM.2017.8247551

Witvliet, B. A., van Maanen, E., Bentum, M. J., Slump, C. H. & Schiphorst, R. (2015). A novel Method for the Evaluation of Polarization and Hemisphere Coverage of HF Radio Noise Measurement Antennas. *2015 IEEE International Symposium on Electromagnetic Compatibility (EMC)*. Dresden, Germany, 6-22 August 2015. https://doi.org/10.1109/ISEMC.2015.7256174